Table I. Carrier-Mediated Transport of AMP and ADP through a Chloroform Liquid Membrane

run	aqueous I nucleotide	aqueous I concn, M	aqueous I pH	$CHCl_3$, **1**, M	aqueous II pH	aqueous II salt, M	transport rate, $\mu M/h \cdot cm^2$
1	ADP	1.0×10^{-2}	8.0	2.5×10^{-4}	0.5		2.62
2	ADP	1.0×10^{-2}	8.0	2.5×10^{-4}	1.0		1.05
3	AMP	1.0×10^{-2}	8.0	2.5×10^{-4}	1.0		0.22
4	ADP	1.0×10^{-2}	5.0	2.5×10^{-4}	0.5		0.238
5	ADP	1.0×10^{-2}	5.0	1.0×10^{-3}	0.5		1.8
6	AMP	1.0×10^{-2}	5.0	2.5×10^{-4}	0.5		0.006
7	ADP	1.0×10^{-3}	5.0	2.5×10^{-4}	5.0	NaBr (1.0×10^{-2})	0.267
8	ADP	5.0×10^{-4}	5.0	2.5×10^{-4}	5.0	[NaBr (1.0×10^{-2})-ADP (5.0×10^{-4})]	0.267

lectively at one interphase of water–chloroform and transported it through a chloroform liquid membrane and released the nucleotide into the other aqueous phase.[5] Proton and salt concentration gradients successfully drove the passive as well as the active transport of AMP and ADP.

Thus, distearyl-Dabco dichloride **1**[4] was dissolved in chloroform (2.5×10^{-4} M, 10 mL) and the solution was stirred gently (rpm, 50) in contact with two aqueous phases, one (aq I) containing adenosine mono- or diphosphate (1.0×10^{-2} M, 5 mL) and the other (aq II) filled with water (5 mL). The pH of each aqueous phase was adjusted by the addition of a small amount of concentrated NaOH or HCl solution to the specified value listed in Table I. The nucleotide concentration in aq II, monitored spectroscopically (λ_{max} 260 nm), increased following zeroth-order kinetics.[6] Transport rates obtained from their slopes are listed in Table I. When comparison was made with rates obtained at the same pH gradients, ADP was transported more effectively than AMP. The transport rate ratio, k_{ADP}/k_{AMP}, was estimated to be 4.8 at pH 8.0 (runs 2 vs. 3) and amounted to 40 at pH 5.0 (runs 4 vs. 6). The higher rate ratio at pH 5 is assignable to the higher selectivity observed for the binding of ADP compared with that ofAMP at pH 5.0.[4] The higher the pH of aq I, the larger was the overall transport rate (runs 1 vs. 4), as expected from the more effective uptake of nucleotide from the aqueous to the organic phase at higher pH. It is worth mentioning here that the transport rate reported here is comparable with that reported by Lehn et al.[3a] for the transport of amino acid by means of phase-transfer reagent tricaprylmethylammonium chloride. Our value is, e.g., 1.05×10^{-2} M/(h·cm²·M carrier) for run 1 and Lehn's ranges from 2.0×10^{-4} for serine to 1.25×10^{-2} for phenylalanine. Note that, in the amino acid transport, much more drastic condition was applied to promote the membrane potential difference, i.e., 0.1 N KOH and 0.1 N HCl and the initial substrate concentration was 5-fold larger than ours.

To suppress the concomitant hydrolysis of ADP in aq II observed during the above slow transport,[7] the transport rate should be accelerated. For the purpose, we examined the relative rate of release of the nucleotide by the exchange with an anion dissolved in aq II. The relative rates of the liberation of ADP bound to **1** were in the following decreasing order: $ClO_4^- > SCN^- > Br^- > NO_3^- > PPi > SO_4^{2-} > Cl^- > HCO_3^- > F^- > CH_3CO_2^- > Pi$. Perchlorate and thiocyanate anions released all of bound ADP very readily but they formed stable complexes with diammonium salt **1** inhibiting any further transport of the nucleotide. Thus, bromide anion was chosen for the exchange reagent in aq II. As shown in run 7, the ADP transport was successfully driven by use of the salt gradient of NaBr without proton gradient. ADP transported did not suffer undesirable hydrolysis to an observable extent.

Active transport of ADP was attempted by using the triphase system where the initial concentrations of ADP were the same (5×10^{-4} M) for both aqueous phases (run 8). The ADP concentration in aq II increased at the same rate as observed for run 7, consistent with the identical decrease rate of ADP in aq I. The result clearly indicates the first successful active transport of nucleotide by means of synthetic carrier molecule. A direct application of this transport device may involve an accumulation of nucleotides which formed in low concentrations via e.g., oxidative or photophosphorylation.

References and Notes

(1) (a) Christensen, H. N. "Biological Transport", 2nd ed.; Benjamin: New York, **1975**; Chapter 10. (b) Shamoo, A. E., Ed. *Ann. N.Y. Acad. Sci.* **1975**, 264. (c) Green, D. E.; Blondin, G.; Kessler, R.; Southard, J. H. *Proc. Natl. Acad. Sci. U.S.A.* **1975**, *72*, 896.

(2) (a) Lehn, J.-M. *Struct. Bonding (Berlin)* **1973**, *16*, 1. (b) Simon, W.; Morf, W. E.; Meier, P. C. *Ibid.* **1973**, *16*, 113. (c) Pressman, B. C. *Annu. Rev. Biochem.* **1976**, *45*, 501. (d) Lehn, J.-M. *Pure Appl. Chem.* **1977**, *49*, 857. (e) Lehn, J.-M. *Acc. Chem. Res.* **1978**, *11*, 49.

(3) (a) Behr, J.-P.; Lehn, J.-M. *J. Am. Chem. Soc.* **1973**, *95*, 6108. (b) Graf, E.; Lehn, J.-M. *Ibid.* **1976**, *98*, 6403. (c) Lehn, J.-M.; Sonveaux, E.; Willard, A. K. *Ibid.* **1978**, *100*, 4914. (d) Dietrich, B.; Fyles, T. M.; Lehn, J.-M.; Pease, L. G. *J. Chem. Soc., Chem. Commun.* **1978**, 934. Although the possible use for anion transport is mentioned in the last three papers, no result is reported on transport therein.

(4) Tabushi, I.; Imuta, J.; Seko, N.; Kobuke, Y. *J. Am. Chem. Soc.* **1978**, *100*, 6287.

(5) The cell used was similar to the one described in ref 3a. The outer area of the interphase (aq I) was 3.43 cm² and the inner (aq II) was 3.65 cm².

(6) When aq I was adjusted to pH 8, an induction period (~50 h) was observed during which the nucleotide concentration in the chloroform phase increased gradually to a steady-state value (1.27×10^{-5} M). The transport rates listed in Table I are values obtained at the steady state. When pH was set to 5.0 in aq I, no appreciable induction period was observed.

(7) Analysis found that 85% of ADP transported was hydrolyzed to AMP after 68 h.

Iwao Tabushi,* Yoshiaki Kobuke, Jun-ichi Imuta

Department of Synthetic Chemistry
Kyoto University, Yoshida, Kyoto 606, Japan

Received July 25, 1979

Resolution and Assignment of the 270-MHz Proton Spectrum of Cellobiose by Homo- and Heteronuclear Two-Dimensional NMR

Sir:

The growing interest in complex naturally occurring carbohydrates encourages the development of methods for the determination of their primary structure and solution geometry. Although conventional ^1H NMR methods have sufficient resolving power to provide detailed structural information for derivatized oligosaccharides which are soluble in organic solvents, studies of oligosaccharides in aqueous solution are largely confined to the anomeric resonances. However, as we now demonstrate for cellobiose (**1**, D-glucopyranosyl-(β1→4)-D-glucopyranose), the combined use of homo- and heteronuclear two-dimensional (2D) NMR[1,2] makes possible a complete resolution and assignment of the proton spectrum.

Standard experimental methods were used to obtain the proton 2D *J* spectrum[3-5] and the carbon-13–proton chemical shift correlation 2D spectrum[2,6] of a 0.3 M solution of cellobiose in D_2O. The 2D *J* spectrum of Figure 1 was obtained by applying[7] a 45° tilt[3,8] to the experimental 2D spectrum, so that the horizontal and vertical frequency axes display pure

0002-7863/80/1502-1745$01.00/0

Table I. ^1H and ^{13}C NMR Parameters for Cellobiose

		1	2	3	4	5	6
^{13}C shift[a]	β-D-glucopyranosyl	103.37	73.97	76.31	70.28	76.80	61.41
	β-D-glucopyranose	96.56	74.70	75.10	79.43	75.60	60.87
	α-D-glucopyranose	92.63	72.04	72.15	79.56	70.92	60.74
^1H shift[b]	β-D-glucopyranosyl	4.52	3.33, 3.32[c]	3.52	3.41	3.51	3.93, 3.74
	β-D-glucopyranose	4.67	3.29	3.63[d]	3.63[d]	3.59[d]	3.96, 3.81
	α-D-glucopyranose	5.23	3.58	3.83	3.65	3.96	3.88[d]

		$J_{1,2}$	$J_{2,3}$	$J_{3,4}$	$J_{4,5}$	$J_{5,6A}$	$J_{5,6B}$	$J_{6A,6B}$
^1H coupling constant[e]	β-D-glucopyranosyl	7.9	9.5	8.8	9.9	2.4	5.8[f]	12.5
	β-D-glucopyranose	7.9	9.5	[g]	[g]	2.3	4.8[f]	12.3
	α-D-glucopyranose	3.8	9.8	8.6	[g]	[g]	[g]	[g]

[a] ±0.02 ppm, referred to external Me_4Si via internal dioxane at δ 67.40. [b] ±0.02 ppm, referred to internal TSP. [c] α,β forms, respectively. [d] Approximate shift; strongly coupled. [e] ±0.3 Hz, signs not determined. [f] Assignment of ref 11 reversed. [g] Strongly coupled multiplet. All values are reported for a 0.3 M solution in D_2O at 22 ± 2 °C.

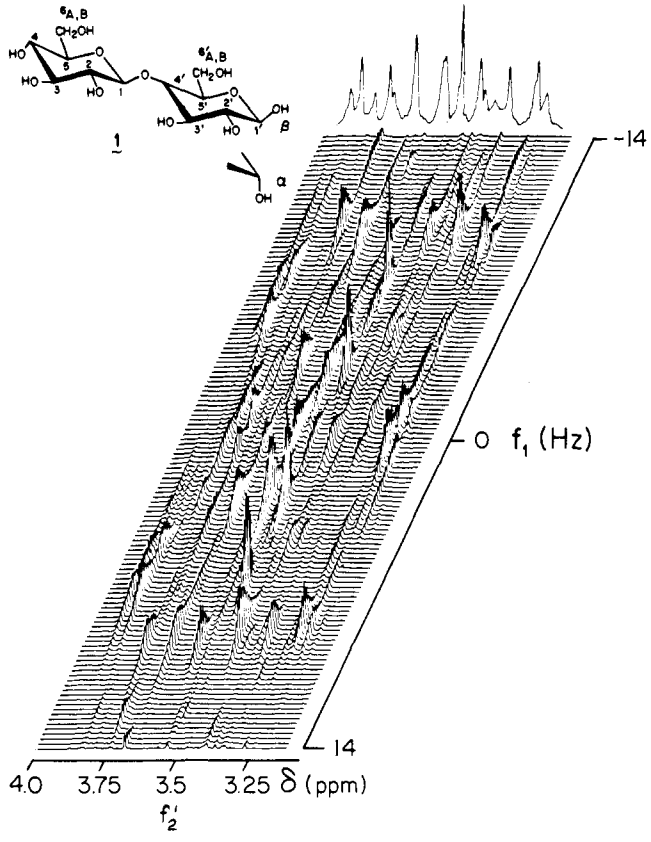

Figure 1. The proton 2D *J* spectrum of cellobiose (**1**), 0.3 M in D_2O, after application of a 45° tilt in frequency space. Projection (digital summation) of this spectrum onto the horizontal (f_2') axis yielded the spectrum of Figure 2A.

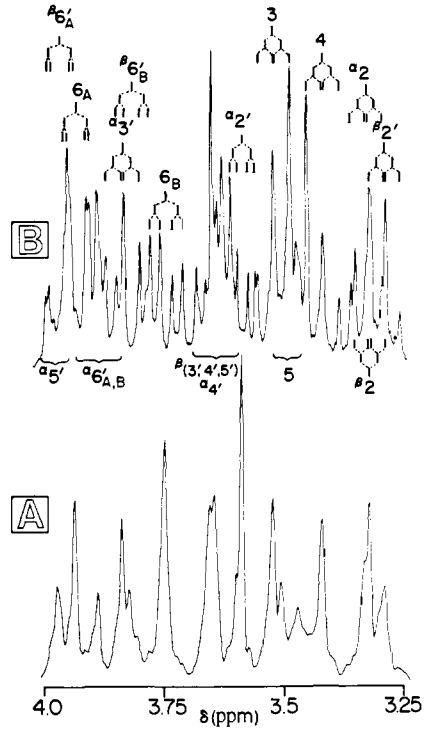

Figure 2. A, the proton spectrum of **1** with all homonuclear couplings suppressed, obtained by projection of the spectrum in Figure 1 onto the f_2' axis; B, the conventional proton spectrum of the nonanomeric resonances of **1**, with assignments made using the data obtained from Figures 1 and 3.

chemical shift and pure multiplet structure respectively. As a result the f_2' projection[9] (Figure 2A) of this 2D spectrum shows a singlet for each proton at its chemical shift, while the f_1 cross section[9] at a given f_2' displays the partial *J* spectrum for that chemical shift. This complete separation (for weakly coupled spin systems) of chemically shifted multiplets provides a fully resolved spectrum; however, in this case the similarity of many of the scalar couplings leaves a considerable assignment problem.

The 2D chemical shift correlation spectrum (Figure 3) displays carbon chemical shift information in f_2 (vertical axis) and proton shifts in f_1 (horizontal axis), one signal appearing for each directly bonded carbon–proton pair. Extraction of cross sections through f_1 at the carbon chemical shift frequencies, assigned previously by Pfeffer and co-workers,[10] allows the proton shifts for each site to be measured with an accuracy of better than 0.05 ppm. This is sufficient to allow the complete assignment of the spectrum in Figure 1, with the results summarized in Table I.

Spectra were obtained on a home-built superconducting spectrometer operating at 270 MHz for protons and 67.9 MHz for carbon-13. Data acquisition took ~60 min for Figure 1 and 60 min for Figure 3, using 5- and 10-mm-diameter sample tubes, respectively. Proton and carbon chemical shifts in Figure 3 are referenced to external Me_4Si; (not shown); in Table I the proton shifts have been corrected to refer to internal DSS. These results are consistent with the partial assignment by 300-MHz CW INDOR of DeBruyn et al.[11]

The use of 2D spectroscopy in the NMR of oligosaccharides, especially the synergistic combination described here, provides a considerable increase in resolving power and information content over that obtainable using conventional methods at the highest spectrometer operating frequencies now available. Indeed, the conventional spectrum of the nonanomeric protons of cellobiose at 270 MHz shown with assignments in Figure

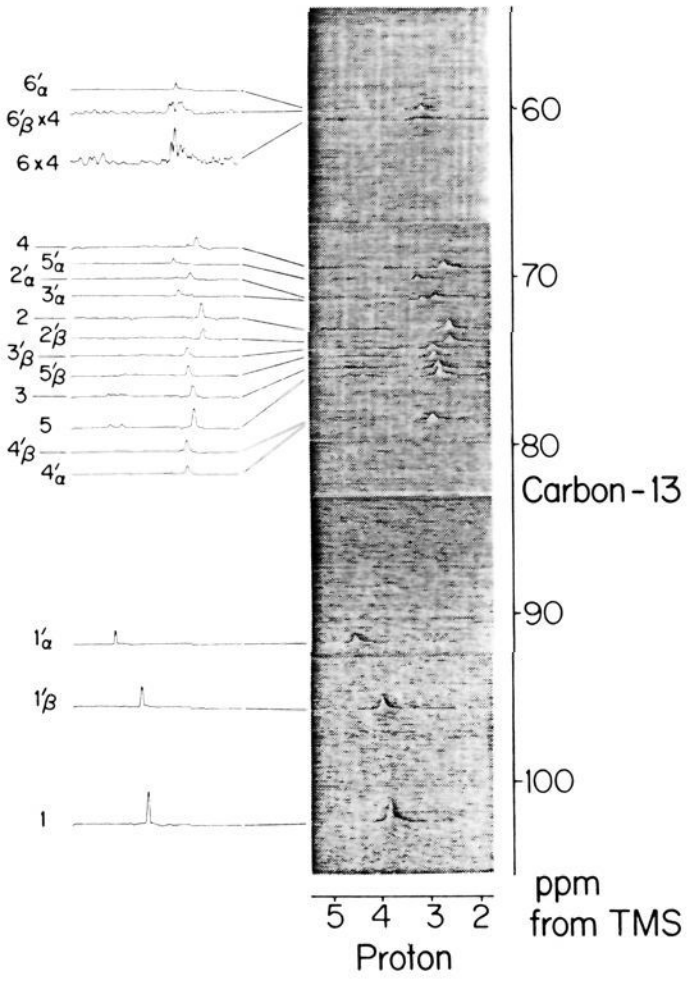

Figure 3. The carbon-13–proton 2D shift correlation spectrum of **1**, again 0.3 M in D_2O, showing carbon-13 chemical shifts in the vertical (f_2) and proton shifts in the horizontal (f_1) frequency axes. Individual zero-filled traces are shown for each of the carbon-13 chemical shifts, allowing the chemical shifts of the directly bound protons to be measured with a precision better than 0.05 ppm, assigned via the carbon shifts of ref 10. The vertical scale was increased fourfold for the 6′β and 6 traces.

2B would still provide a considerable analysis problem even if it were measured at a proton frequency of 1 GHz, well beyond the limits of present NMR technology. It is important to note that the signals in the shift correlation experiment are governed by proton spin population differences and relaxation times (except the unmodulated carbon signals) which enhances the sensitivity of the technique. We emphasize that the total amounts of machine time required are by no means prohibitive, and the experiments can be performed on a "routine" basis.

Acknowledgments. This work was supported by an operating grant from the National Science and Engineering Research Council of Canada (A1905 to L.D.H.). Thanks are due to the Izaak Walton Killam Foundation for the award of a postdoctoral research fellowship to G.A.M., and to UBC for a summer stipend (S.S.).

References and Notes

(1) Aue, W. P.; Bartholdi, E.; Ernst, R. R. *J. Chem. Phys.* **1976,** *64,* 2229.
(2) Freeman, R.; Morris, G. A. *Bull. Magn. Reson.* **1979,** *1,* 5.
(3) Aue, W. P.; Karhan, J.; Ernst, R. R. *J. Chem. Phys.* **1976,** *64,* 4226.
(4) Bodenhausen, G.; Freeman, R.; Morris, G. A.; Turner, D. L. *J. Magn. Reson.* **1978,** *31,* 75.
(5) Hall, L. D.; Sukumar, S.; Sullivan, G. R. *J. Chem. Soc., Chem. Commun.* **1979,** 292.
(6) Freeman, R.; Morris, G. A. *J. Chem. Soc., Chem. Commun.* **1978,** 684.
(7) Hall, L. D.; Morris, G. A.; Sukumar, S. *Carbohydr. Res.,* **1979,** *76,* C7.
(8) Nagayama, K.; Wüthrich, K.; Bachmann, P.; Ernst, R. R. *Naturwissenschaften* **1977,** *64,* 581.
(9) Nagayama, K.; Bachmann, P.; Wüthrich, K.; Ernst, R. R. *J. Magn. Reson.* **1978,** *31,* 133.
(10) Pfeffer, P. E.; Valentine, K. M.; Parrish, F. W. *J. Am. Chem. Soc.* **1979,** *101,* 1265.
(11) DeBruyn, A.; Anteunis, M.; Verhegge, G. *Bull. Soc. Chim. Belg.* **1974,** *84,* 721.

Laurance D. Hall,* Gareth A. Morris, Subramaniam Sukumar
Department of Chemistry, University of British Columbia
Vancouver, British Columbia, Canada V6T 1W5
Received August 7, 1979

Heterobimetallic Hydrogen Transfer in the Reduction of Metal Acyl Complexes

Sir:

Several groups have demonstrated the ability of certain early transition metal complexes to activate carbon monoxide towards reduction by hydrogen.[1] Stoichiometric reactions produce methane or coordinated methoxide or enediols. A major obstacle to the anticipated catalytic utilization of such reactions is the formation of metal–oxygen bonds which are resistant to reduction by H_2. One solution to this problem might be found among the less oxophilic metals further to the right in any transition series.[2] Labinger[3] has pointed out, however, that the hydride complexes of such metals lack the "hydridic" reactivity which is claimed[1a] to be important in effecting CO reduction. We report here that several such "impotent" hydrides are in fact quite capable of hydrogenating a particular class of metal acyl complexes, a reaction which is a probable component in CO hydrogenation reactions.

Acyl complex I forms readily (1 atm, 25 °C) from CO and $Cp_2Zr(CH_3)_2$.[4] It is unreactive toward H_2 (1 atm, overnight); however, I reacts with Cp_2MoH_2 in the time of mixing (C_6D_6, 25 °C) to produce $Cp_2Zr(CH_3)OCH_2CH_3$.[5] This reaction

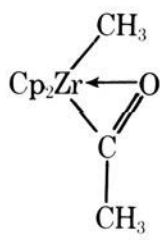

I

sequence, which represents reduction of CO to the alkoxide oxidation level, is completely selective, there being no evidence for any hydrogen transfer to the $Zr–CH_3$ group.[6] The isotopomer $Cp_2Zr(CH_3)OCD_2CH_3$ is formed when Cp_2MoD_2 is employed; no hydrogen scrambling between the methyl and methylene protons occurs under these mild conditions. The high rate of this reaction is remarkable in view of the instability of the possible product fragment "Cp_2Mo", and the fate of this unit is of some interest. If the reaction is performed under 1 atm of CO, the molybdenum is transformed predominantly to Cp_2MoCO. In CD_3CN, the observed spectra are consistent with the product being $Cp_2Mo(NCCD_3)$.[7] Under molecular nitrogen in C_6D_6, Cp_2MoCO remains a major product, being formed by facile decarbonylation[4] of I to $Cp_2Zr(CH_3)_2$; this dimethyl compound is unreactive toward Cp_2MoH_2 at 25 °C. Quantitative measurements of the reaction stoichiometry establish that, under dinitrogen, 1 mol of Cp_2MoH_2 produces in excess of 1 mol of $Cp_2Zr(CH_3)OCH_2CH_3$. This observation may be accommodated by assuming ring to molybdenum hydrogen migration at some stage of the mechanism, followed by transfer of this new hydrogen to I. In accord with this contention, a second molybdenum-containing product is formed which exhibits a complex ^1H NMR pattern characteristic of both η^5-C_5H_5 and C_5H_4X units; we have identified this product as II by comparison with an authentic sample.[8] Hydrogen

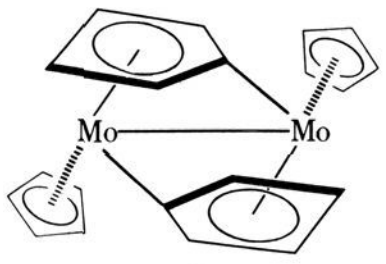

II

transfer from Cp_2MoH_2 to $Cp_2ZrCl[\eta^2$-$C(O)CH_3]$[9] is again specific to the acyl group, no metathesis of Cl for H on zirconium being observed. This acyl is more resistant to decarbonylation than I in the hydrogen-transfer reaction, and con-

0002-7863/80/1502-1747$01.00/0